

Dielectric Breakdown Mechanism of Perovskite-Structured Ceramics

Takuya Hoshina, Mikio Yamazaki, Hiroaki Takeda, and Takaaki Tsurumi
 Tokyo Institute of Technology
 2-12-1 Ookayama, Meguro, Tokyo, 152-8552, Japan
 Phone: 81-3-5734-2520, e-mail: thoshina@ceram.titech.ac.jp

Abstract

We precisely measured the dielectric breakdown strength of SrTiO₃, CaTiO₃, and CaZrO₃ ceramics as a function of temperature, and revealed the dielectric breakdown mechanism of the ceramics. For the dielectric breakdown test, ceramics specimens with a lot of round-bottom holes were prepared. Using the specimens, the breakdown positions were stabilized and a reliability of breakdown strength was improved as well as the measurement efficiency. As a result of the dielectric breakdown tests, it was found that the dielectric breakdown strength decreased with increasing permittivity at room temperature and the permittivity dependence of breakdown strength obeyed Griffith type energy release rate model. At high temperature above 100°C, the dielectric breakdown mechanism of SrTiO₃ and CaTiO₃ ceramics was explained by an intrinsic breakdown model. In contrast, an intrinsic dielectric breakdown of CaZrO₃ ceramics didn't occur in the measurement temperature range up to 210°C. To obtain a high dielectric breakdown strength at high temperature, the dielectric permittivity is required to be low to some extent and the defect concentration of oxygen vacancies should be minimized in the perovskite-structured oxide.

Key words: dielectrics, breakdown, permittivity, high-power

Introduction

The commercialization of power modules for high power and high temperature applications has been strongly promoted in recent years. In order to realize a next-generation SiC-based power circuits, it is necessary to develop passive components useful at high temperatures up to 200°C and high voltages up to 600 V. A challenge is to replace the snubber capacitors in inverter circuits from conventional organic film capacitors to multilayer ceramics capacitors (MLCCs). For downsizing snubber-MLCCs, both of permittivity and breakdown strength of dielectrics used in the MLCCs should be as high as possible. Therefore it is necessary to understand the relationship between the dielectric permittivity and dielectric breakdown strength, and reveal the temperature dependence of breakdown strength.

Recently, the Griffith type energy release rate model has been proposed to explain the dielectric breakdown of bulk ceramics.^{1,2} According to the Griffith type model, the dielectric breakdown strength decreases with increasing permittivity, whereas it is independent of temperature. However, it is known that the dielectric breakdown strength is generally affected by temperature change.^{3,4}

In this study, we precisely measured the dielectric breakdown strength as a function of temperature for several kinds of perovskite-structured ceramics, and revealed the dielectric breakdown mechanism of the

ceramics.

Experimental

SrTiO₃, CaTiO₃, and CaZrO₃ ceramics were selected as specimens to measure the dielectric breakdown strength. Raw powders of SrTiO₃, CaTiO₃, and CaZrO₃ (Sakai Chemical Industry, particle size: 300 nm) were respectively mixed with polyvinyl acetate for 20 h by ball-milling. After milling, the powders were isostatically pressed at 100 MPa for 1 min. The resulting green compacts were sintered by a conventional sintering and two-step sintering processes.^{5,6} to control the grain sizes. The green compacts of SrTiO₃ and CaZrO₃ were heated to 1500°C at 5°C/min and isothermally sintered for 4 h. On the other hand, the green compacts of CaTiO₃ were heated to $T_1 = 1390^\circ\text{C}$ at 10°C/min, immediately cooled to lower temperatures ($T_2 = 1270^\circ\text{C}$) at 10°C/min, and isothermally sintered for 4 h. The obtained ceramics were characterized using the following methods. The densities of the ceramics were measured by the Archimedes method. Average grain sizes were estimated using a scanning electron microscopy (SEM; JEOL JCM-6000). The crystal structures were investigated by X-ray diffraction (XRD) measurement (Rigaku RINT2000, Cu K α , 50 kV, 40 mA). The dielectric permittivities were measured using an impedance analyzer (Agilent 4294A) after depositing

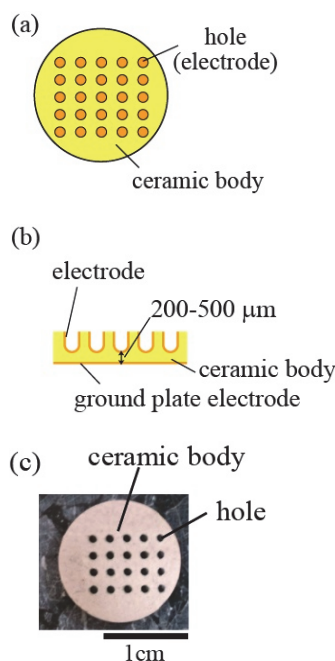


Fig. 1. Schematic illustrations of (a) surface and (b) cross-section of test specimen for dielectric breakdown test. (c) Photograph of CaTiO_3 ceramics prepared for dielectric breakdown test.

Au electrodes on the top and bottom surfaces by DC sputtering. In addition, polarization–electric field (P – E) curves were measured using a ferroelectric test system (Radiant, Precision LC) at 100 Hz.

The measurement of dielectric breakdown strength is usually time-consuming work because the dielectric breakdown strength is probabilistically estimated by Weibull statistical analysis, which demands a large number of accumulations of experimental data.⁷ If the number of measurement data is not enough, the breakdown strength may not be correctly estimated due to the variation in the data. To improve the efficiency of measurement, we developed a system to evaluate dielectric breakdown strength of ceramics in this study. **Figure 1** shows the shape of the test specimen for our measuring technique. The specimen had a lot of round-bottom holes, where the dielectric breakdown tests were performed. We could accumulate a lot of data enough for Weibull analysis from a small number of specimens. Moreover, the electric field was converged at the bottom of hole, which stabilized the breakdown positions in a specimen. The shape preventing a creeping discharge and partial discharge provided more accurate breakdown strength data with little dispersion. The holes were formed on the surface of green body using a ball end mill with a diameter of 1 mm. After

sintering, the back side of specimen was polished for reducing the thickness of specimen. The inside of holes and the back side of specimen were electroded with Au sputtering. The dielectric breakdown test was performed in silicone oil (Shin-etsu chemical KF96-1000cs) at -30 – 210°C . DC voltage was applied to the specimen using a high withstanding voltage tester (Keisoku Giken 7474). The applied voltage and leakage current were recorded on a computer during breakdown test. At least 7 breakdown tests were performed for each sample to conduct Weibull statistical analysis. The Median rank method was applied with a fracture probability in Weibull plot.

Results and Discussion

The obtained ceramics samples of SrTiO_3 , CaTiO_3 , and CaZrO_3 had high relative densities over 94%. **Figure 2** shows relative permittivities (ϵ_r) and dielectric loss tangents ($\tan\delta$) of SrTiO_3 , CaTiO_3 , and CaZrO_3 ceramics at 30 – 210°C and 1 kHz. At 30°C , the relative permittivities of SrTiO_3 , CaTiO_3 , and CaZrO_3 were 273, 173, and 30, respectively. SrTiO_3 , CaTiO_3 , and CaZrO_3 indicate paraelectric state at 30°C and don't have phase transition at 30 – 210°C . Therefore, the permittivity should originally decrease with increasing temperature in accordance with the Curie-Weiss law. In **Fig. 2**, the permittivity of CaTiO_3 ceramics seems to increase with increasing temperature above 130°C , however, the increase is due to high dielectric loss at high temperature. For the CaTiO_3 and SrTiO_3 ceramics, the dielectric loss increased with increasing temperature above 100°C , which meant that CaTiO_3 and SrTiO_3 ceramics had low insulation at high temperature. From the measurement of P – E curves, it was confirmed that SrTiO_3 , CaTiO_3 , and CaZrO_3 ceramics were linear dielectrics, which meant the permittivities of SrTiO_3 , CaTiO_3 , and CaZrO_3 ceramics were constant independently of the electric field.

In the dielectric breakdown measurement, a lot of round-bottom holes were formed on the surface of a ceramics body in order to converge the electric field at the bottom of holes and stabilize breakdown position in the specimen. It is known that the electric field changes depending on the electrode geometry, e.g. the shape of hole, and the distance between the bottom of hole and ground plane electrode (to be referred as specimen thickness (d)). The maximum electric field at the bottom of hole (E_m) generally expressed as

$$E_m = M \times V / d, \quad (1)$$

where M is the factor of electric field convergence, and V is the applied voltage. The convergence factor M is a function of specimen thickness d while it is unity for plate-shaped specimen. To estimate the electric field E_m , the factor M was calculated by finite element method (FEM) as shown in **Fig. 3**. **Fig. 3(b)** shows the

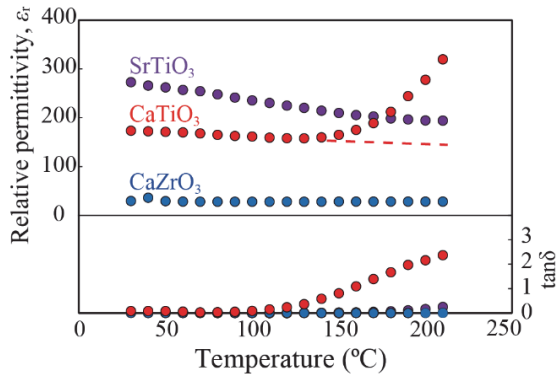


Fig. 2. Dielectric properties of SrTiO₃, CaTiO₃, and CaZrO₃ ceramics as a function of temperature.

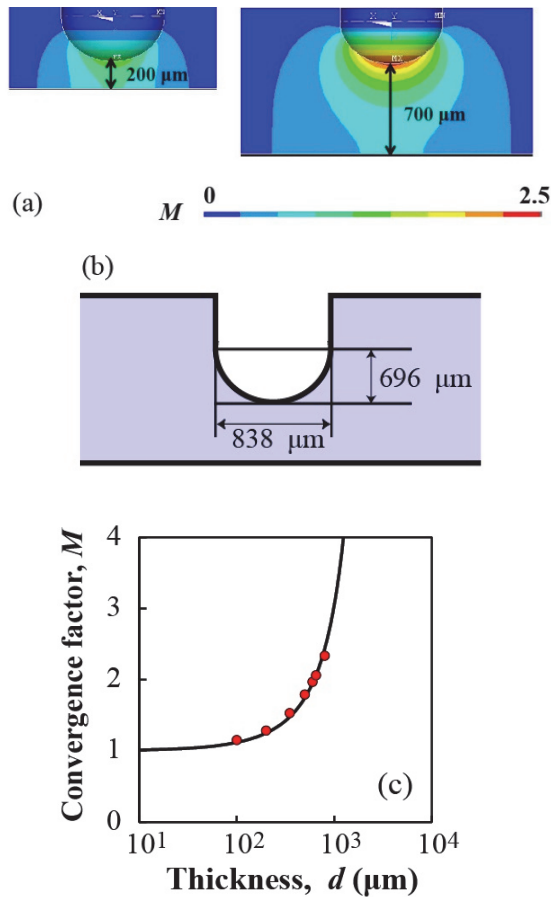


Fig. 3. (a) FEM simulation of electric field convergence factor M for specimen thickness of 200 and 700 μm . (b) Specimen's configuration in FEM which was decided by cross-sectional observation using SEM. (c) Electric field convergence factor as a function of specimen thickness.

shape of hole for the CaTiO₃ specimen. The shape was decided by cross-sectional observation using SEM. Fig. 3(c) shows the relationship between the convergence factor M and specimen thickness d for the CaTiO₃ specimen. The convergence factor increased with increasing specimen thickness. From the relationship of Fig. 3(c) and the specimen thickness estimated by SEM observation, the maximum electric field E_m was determined.

Figure 4 shows the Weibull plots of dielectric breakdown strength for the CaTiO₃ ceramics. Provided that a fracture probability is 50%, the relationship between the breakdown strength and permittivity at room temperature was obtained, as shown in Fig. 5. Compared with literature data (Ref. 2), both our result and literature data showed that the breakdown strength decreased with increasing permittivity. G. A. Schneider and co-worker have explained the dielectric breakdown mechanism by the Griffith type energy release rate model.^{1,2} This model assumes electrically conducting filaments on the surface of specimen. When the applied voltage reaches the breakdown voltage, one of these conducting filaments starts to grow unstably and create the breakdown channel. The breakdown strength due to the Griffith type energy release rate model is given as

$$E_{\text{Griffith}} = \frac{1}{c} \sqrt{\frac{6G_b}{5\pi\epsilon_r\epsilon_0 da_{\text{bd}}}}, \quad (2)$$

where c is constant, G_b is the breakdown toughness, ϵ_r and ϵ_0 are respectively relative permittivity and permittivity of free space, d is the specimen thickness, and a_{bd} is the length of the conducting filament. As shown in **Fig. 5**, the breakdown strength was proportional to the -0.5 power of permittivity. Moreover, a through crack, which is one of the features of Griffith-type breakdown, was observed at the electric field concentrated part after the dielectric breakdown test at room temperature. Therefore, the dielectric breakdown mechanism at room temperature could be explained by the Griffith type energy release rate model.

Figure 6 shows the temperature dependences of breakdown strength for SrTiO₃, CaTiO₃, and CaZrO₃ ceramics. The breakdown strength of CaZrO₃ ceramics shown in Fig. 6(c) was independent of temperature. In addition, a through crack was observed in the CaZrO₃ ceramics after the dielectric breakdown over the entire temperature range of 30–210°C. Therefore, the dielectric breakdown of CaZrO₃ ceramics at 210°C or lower is explained by the Griffith type energy release rate model. In contrast, for SrTiO₃ and CaTiO₃ ceramics, the breakdown strength decreased with increasing temperature above 100°C. This result suggested that the breakdown strength of

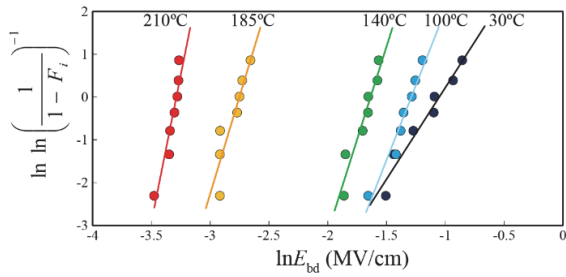


Fig. 4. Weibull plots of dielectric breakdown strength for the CaTiO_3 ceramics.

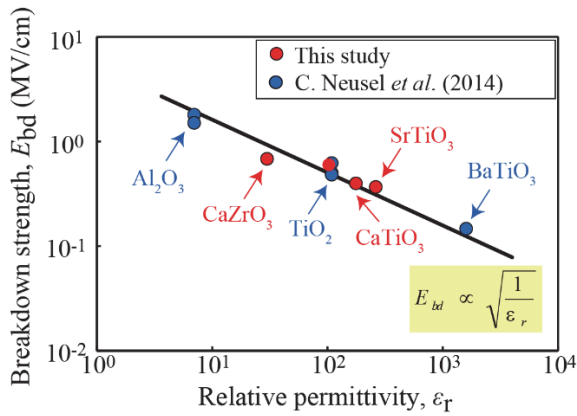


Fig. 5. Relationship between dielectric breakdown strength and permittivity.

SrTiO_3 and CaTiO_3 ceramics at the high temperature above 100°C didn't obey the Griffith model in which the breakdown strength is independent of temperature. **Figure 7** shows leakage current of SrTiO_3 and CaTiO_3 ceramics under the breakdown voltage. The leakage current of SrTiO_3 and CaTiO_3 ceramics significantly increased with increasing temperature at the temperature above 100°C , while it was quite small at the temperature below 75°C . Moreover, a through crack was never observed in the SrTiO_3 and CaTiO_3 ceramics after the dielectric breakdown at the high temperature above 100°C . Therefore, we thought that the dielectric breakdown of SrTiO_3 and CaTiO_3 ceramics at the high temperature was caused by carrier conduction. There are two types of dielectric breakdown mechanisms caused by carrier conduction, i.e., intrinsic and thermal breakdowns. The breakdown strength (E_i) due to intrinsic breakdown is simplified as

$$E_i = CN^2 \left(\exp\left(\frac{\hbar\omega}{k_B T}\right) - 1 \right)^{-\frac{1}{2}} \exp\left(\frac{\Delta V}{2k_B T}\right), \quad (3)$$

where C is a constant, N is donor density, \hbar is Dirac's constant, ω is angular frequency, k_B is the Boltzmann constant, ΔV is the energy gap from impurity level to

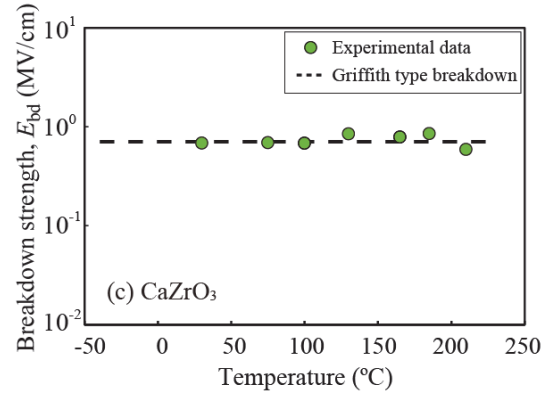
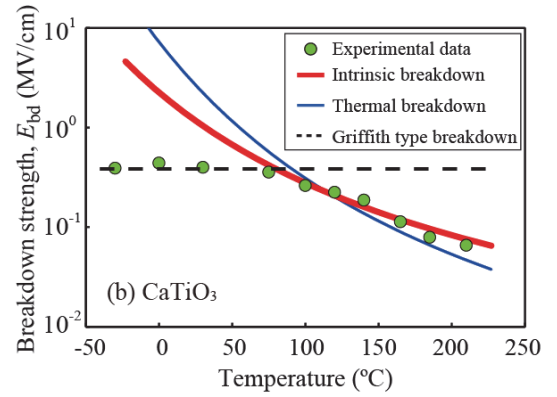
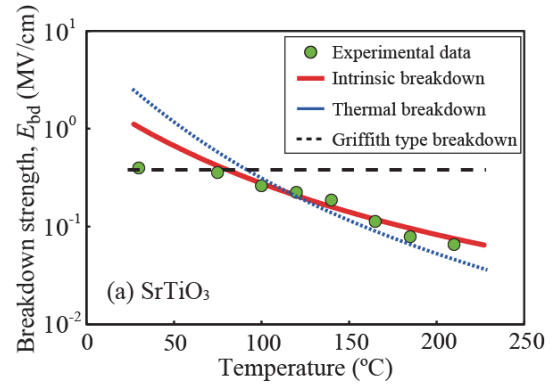


Fig. 6. Dielectric breakdown strength of (a) SrTiO_3 , (b) CaTiO_3 , and (c) CaZrO_3 ceramics as a function of temperature.

the conduction band, and T is temperature. The breakdown strength (E_{th}) due to thermal breakdown is given as follows:

$$E_{th} \cong \sqrt{\left(\frac{3C_v k_B T^2}{\sigma_0 \alpha \tau}\right)} \exp\left(\frac{\Delta V}{2k_B T}\right), \quad (4)$$

where C_v is specific heat at constant volume, σ_0 is conductivity at an infinite temperature, α is a constant, and τ is the time to the breakdown. **Figure 8** shows Arrhenius plot of DC conductivity (σ_{DC}) for SrTiO_3 and CaTiO_3 ceramics. From the Arrhenius plot, the energy gaps (ΔV) of SrTiO_3 and CaTiO_3 was estimated

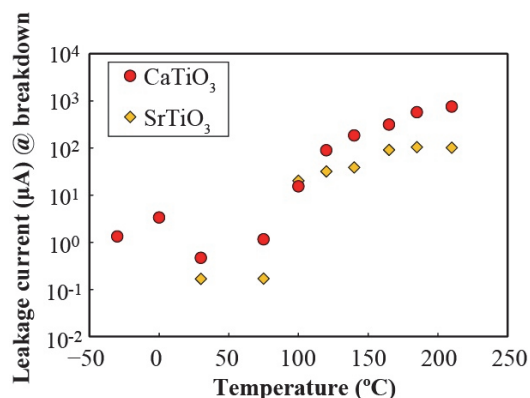


Fig. 7. Leakage current of SrTiO₃ and CaTiO₃ ceramics under the breakdown voltage.

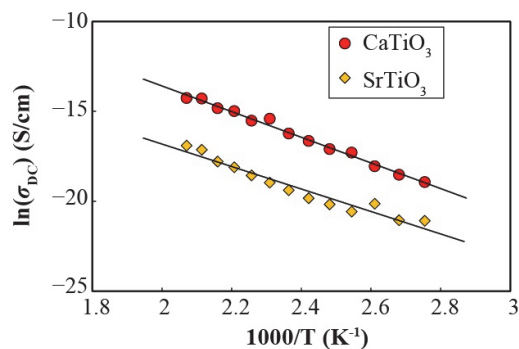


Fig. 8. DC conductivity of SrTiO₃ and CaTiO₃ ceramics as a function of temperature.

to be 0.54 and 0.61 eV, respectively. The energy gaps were close to the energy level of oxygen vacancies in perovskite oxide system.⁸ Therefore the electrical conduction of SrTiO₃ and CaTiO₃ ceramics initiated from the generation of electrons released from oxygen vacancies. Using the energy gaps estimated by the Arrhenius plot, the breakdown strength in the high temperature region was fitted by Eqs. (3) and (4) as shown in Fig. 6(a) and 6(b). Better fitting results could be obtained by the intrinsic breakdown model (Eq. (3)), suggesting that the intrinsic breakdown model describes the dielectric breakdown mechanism of SrTiO₃ and CaTiO₃ ceramics at the high temperature above 100°C.

For the SrTiO₃ and CaTiO₃ ceramics, the low-temperature and high-temperature breakdown mechanisms were explained by the Griffith type energy release rate model and intrinsic breakdown model, respectively. At a low temperature, the E_{Griffith} is lower than the E_i , therefore the breakdown strength is determined by the E_{Griffith} . At a high temperature, the E_i becomes lower than the E_{Griffith} with increasing carrier conduction, and then the intrinsic breakdown

becomes dominant mechanism of dielectric breakdown. Because the intrinsic breakdown initiated from the generation of electrons released from oxygen vacancies, the E_i can be increased by reducing oxygen vacancies in the perovskite-structured oxide. It is known that the formation energy of oxygen vacancy in CaZrO₃ is higher than that in SrTiO₃ and CaTiO₃. Therefore, it is supposed that the defect concentration of oxygen vacancies in CaZrO₃ ceramics was lower than that in SrTiO₃ and CaTiO₃ ceramics. This means that the E_i of CaZrO₃ is higher than the E_i of SrTiO₃ and CaTiO₃, that is why an intrinsic dielectric breakdown of CaZrO₃ ceramics didn't occur in the measurement temperature range. To obtain a high dielectric breakdown strength at high temperature, the dielectric permittivity is required to be low to some extent and the defect concentration of oxygen vacancies should be minimized in the perovskite-structured oxide.

References

- [1] G. A. Schneider, "A Griffith type energy release rate model for dielectric breakdown under space charge limited conductivity", *J. Mech. Phys. Solids*, Vol. 61, pp. 78–90, September, 2012.
- [2] C. Neusel and G. A. Schneider, "Size-dependence of the dielectric breakdown strength from nano- to millimeter scale", *J. Mech. Phys. Solids*, Vol. 63, pp. 201–213, February, 2014.
- [3] Y. Zhou, P. Yan, N. Yoshimura, Z. Cheng, X. Liang, and Z. Guan, "Depressed DC Breakdown Phenomena near Curie Temperature of BaTiO₃-Based Ceramic Capacitors", *Jpn. J. Appl. Phys.*, Vol. 40, pp. 2336–2340, April, 2001.
- [4] P. H. Fang and W. S. Brower, "Temperature Dependence of the Breakdown Field of Barium Titanate", *Phys. Rev.*, Vol. 113, pp. 456–458, January, 1959.
- [5] I.-W. Chen and X.-H. Wang, "Sintering Dense Nano-Crystalline Ceramics Without Final Stage Grain Growth", *Nature*, Vol. 404, pp. 168–171, March, 2000.
- [6] T. Hoshina, Y. Kigoshi, T. Furuta, H. Takeda, and T. Tsurumi, "Shrinkage Behaviors and Sintering Mechanism of BaTiO₃ Ceramics in Two-Step Sintering", *Jpn. J. Appl. Phys.*, Vol. 50, pp. 09NC07-1–4, September, 2011.
- [7] Y. Wang, Y. C. Chan, Z. L. Gui, D. P. Webb, and L. T. Li, "Application of Weibull distribution analysis to the dielectric failure of multilayer ceramic capacitors", *Mater. Sci. Eng. B*, Vol. 47, pp. 197–203, June, 1997.
- [8] S. Sarangi, T. Badapanda, B. Behera, and S. Anwar, "Frequency and temperature dependence dielectric behavior of barium zirconate titanate nanocrystalline powder obtained by mechano- chemical synthesis", *J Mater Sci: Mater. Electron.*, Vol. 47, pp. 4033–4042, July, 2013.